ADVANCED FUNCTIONAL MATERIALS

FULL PAPER

DOI: 10.1002/adfm.200600489

Accurate Measurement and Characterization of Organic Solar Cells**

By *Vishal Shrotriya*, *Gang Li*, *Yan Yao*, *Tom Moriarty*, *Keith Emery*,* and *Yang Yang**

Methods to accurately measure the current–voltage characteristics of organic solar cells under standard reporting conditions are presented. Four types of organic test cells and two types of silicon reference cells (unfiltered and with a KG5 color filter) are selected to calculate spectral-mismatch factors for different test-cell/reference-cell combinations. The test devices include both polymer/fullerene-based bulk-heterojunction solar cells and small-molecule-based heterojunction solar cells. The spectral responsivities of test cells are measured as per American Society for Testing and Materials Standard E1021, and their dependence on light-bias intensity is reported. The current–voltage curves are measured under 100 mW cm^{-2} standard AM 1.5 G (AM: air mass) spectrum (International Electrotechnical Commission 69094-1) generated from a source set with a reference cell and corrected for spectral error.

1. Introduction

Organic solar cells have attracted much attention in the last several years and today are considered a promising source for clean and renewable energy.[1–6] Organic solar cells are divided into two main categories: ones based on conjugated polymers are the so-called bulk-heterojunction (BHJ) solar cells,[7,8] and the others based on small organic molecules are bilayer heterojunction structures.[9] In polymer-based BHJ solar cells, the most common donor polymers that have been used in the past are poly[2-methoxy-5-(3,7-dimethyloctyloxy)-1,4-phenylene vinylene] (MDMO-PPV),[10–12] regioregular poly(3-hexylthiophene) (RR-P3HT),[13–20] and poly[2-methoxy-5-(2′-ethylhexyoxy)-1,4-phenylene vinylene] (MEH-PPV).[7,21,22] The most common candidate for the acceptor material is [6,6]-phenyl C_{61}-butyric acid methyl ester (PCBM).[23] On the other hand, several small molecules such as copper phthalocyanine (CuPc),[24–26] zinc pthalocyanine (ZnPc),[27,28] tetracene,[29] and pentacene[30] have been used as donors combined with buckminsterfullerene (C_{60}) molecules in a bilayer heterojunction. The highest power conversion efficiency (PCE) reported so far for polymer BHJ solar cells is close to 5 %, for devices based on P3HT.[18–20] For small-molecule-based solar cells, efficiencies up to 6.0 % have been reported for devices based on CuPc.[25] As a result of continuing research efforts, the efficiencies of organic solar cells are now fast approaching the levels where they could be put into commercial applications. For the healthy development of this technology, it is now critical to accurately determine the efficiency values to enable a fair comparison of results from different research groups. Significant efforts have been made in the past to accurately determine the efficiency of solar cells, and a standard test method has been established.[31–33] In 1980 the Cell Performance Laboratory was established by the US Department of Energy at the National Renewable Energy Laboratory (NREL) to provide the US terrestrial photovoltaics community with standardized efficiency measurement and reference-cell calibrations. In the early 1980s similar laboratories were being set up in Germany, Japan, and elsewhere. In the 1980s US and international standards were developed and adopted by the national photovoltaic (PV) calibration laboratories around the world.[32,33] Unfortunately, for organic solar cells, these internationally accepted norms are seldom followed at the research level, partially due to lack of awareness of these norms, limited resources, and/or relatively low efficiency. As a result, efficiency values under various testing conditions have been reported, which makes reliable comparison between data from different research groups very difficult. Some efforts in the past have sought to motivate the organic-solar-cell community toward adopting standards for accurately measuring efficiency.[34,35] In this paper, the research group at the University of California, Los Angeles has collaborated with the NREL to present a simple method to accurately determine the efficiency of organic solar cells. Different kinds of test-cell/reference-cell combinations have been used to calculate the spectral-mismatch factors under the standard refer-

[*] Dr. K. Emery, T. Moriarty
National Renewable Energy Laboratory
Golden, CO 80401 (USA)
E-mail: keith_emery@nrel.gov
Prof. Y. Yang, V. Shrotriya, Dr. G. Li, Y. Yao
Department of Materials Science and Engineering
University of California, Los Angeles
Los Angeles, CA 90095 (USA)
E-mail: yangy@ucla.edu

[**] V. Shrotriya and G. Li contributed equally to this work. The authors thank Douglas Sievers for helpful technical discussions. We also thank Dr. Chih-Wei Chu for helping us with device fabrication. The financial support for this research work was provided by the Office of Naval Research (N00014-01-1-0136, Program Manager Dr. Paul Armistead), and the Air Force Office of Scientific Research (F49620-03-1-0101, Program Manager Dr. Charles Lee). The work by NREL coauthors was performed under DOE contract DE-AC36-99-GO10337.

ADVANCED FUNCTIONAL MATERIALS

ence spectrum. The importance of choosing a suitable reference cell for light-source intensity calibration is also demonstrated. The spectral responsivity measurements are performed on various types of test cells, and the effect of light-bias intensity on external quantum efficiency of organic solar cells is discussed.

2. Rating Organic-Solar-Cell Performance

In this manuscript two types of organic solar cells are focused on for the purpose of accurate efficiency measurement and characterization: i) polymer/fullerene BHJ cells and ii) small-organic-molecule-based bilayer cells. Typical device structures of the two types of cells are shown in Figure 1. Also shown are the chemical structures of the active materials used in the study. The details of the fabrication procedure for both the polymer as well as the small-molecule-based PV cell are provided in the Experimental section. Two different P3HT:PCBM blend solutions were prepared—one with a 1:1 weight ratio (20 mg mL^{-1} P3HT) in 1,2-dichlorobenzene (DCB) and one with a 1:0.8 weight ratio (10 mg mL^{-1} P3HT) in chlorobenzene (CB)—to fabricate two types of polymer BHJ devices named P3HT:PCBM(DCB) and P3HT:PCBM(CB), respectively. Polymer BHJ solar cells using MEH-PPV were also fabricated. For small-molecule-based devices, CuPc was selected as the active layer. The encapsulated devices were brought to NREL to test their current–voltage (I–V) characteristics and measure their external quantum efficiency (EQE) values.

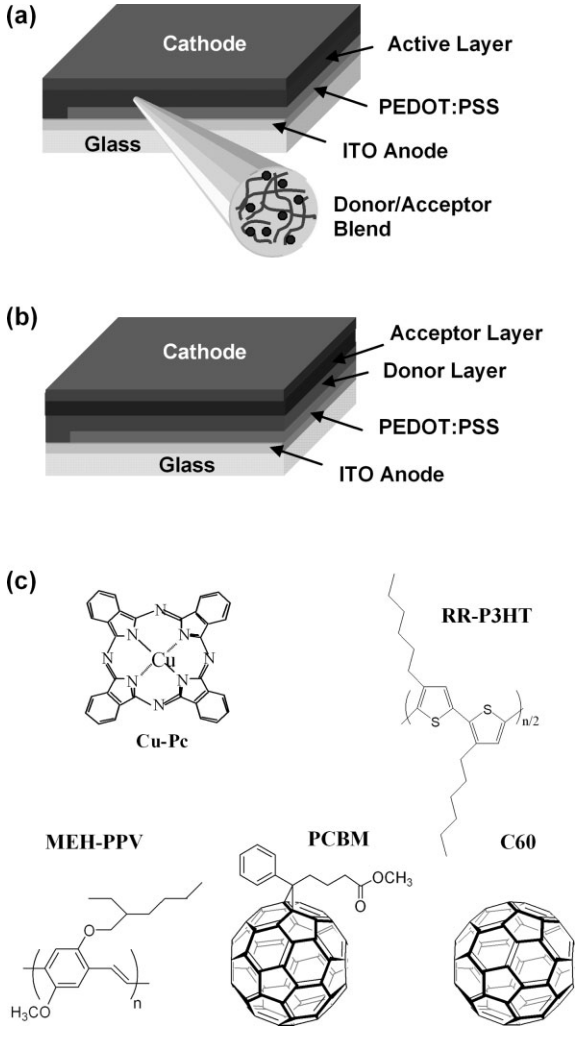

Figure 1. Typical device structures of the a) polymer/fullerene BHJ solar cell and b) small-molecule donor–acceptor heterojunction solar cell (PEDOT: poly(3,4-ethylenedioxythiophene); PSS: poly(styrene sulfonic acid); ITO: indium tin oxide). c) Chemical structures of the active materials used in this work.

The performance of PV cells is commonly rated in terms of their efficiency with respect to standard reporting conditions (SRC) defined by temperature, spectral irradiance, and total irradiance.[33] The SRC for rating the performance of terrestrial PV cells are the following: 1000 W m^{-2} irradiance, AM 1.5 (AM: air mass) global reference spectrum, and 25 °C cell temperature.[36–40] The PCE (η) of a PV cell is given as

$$\eta = \frac{P_{\max}}{E_{\text{tot}} A} 100 \tag{1}$$

where $P_{\max}$ is the measured peak power of the cell, A is the device area, and E_{tot} is the total incident irradiance. For Equation 1 to give a unique efficiency, E_{tot} must be with respect to a reference spectral irradiance. The current reference spectrum adopted by the international terrestrial photovoltaics community is given in International Electrotechnical Commission (IEC) Standard 60904-3 and American Society for Testing and Materials (ASTM) Standard G159.[36,38] A recent improvement to this spectrum is given in ASTM Standard G173 and is expected to be adopted by the international photovoltaics community in the next year or two.[39] The irradiance incident on the PV cell is typically measured with a reference cell. For I–V measurements with respect to a reference spectrum, there is a spectral error in the measured short-circuit current (I_{SC}) of the PV cell because of the following two reasons: i) the spectral irradiance of the light source does not match the reference spectrum, which is computer generated, and ii) the spectral responses of the reference detector and test cell are different. This error can be derived based upon the assumption that the photocurrent is the integral of the product of cell responsivity and incident spectral irradiance. This error can be expressed as spectral mismatch correction factor (M),[41,42]

$$M = \frac{\int_{\lambda_1}^{\lambda_2} E_{\text{Ref}}(\lambda) S_{\text{R}}(\lambda) \mathrm{d}\lambda \int_{\lambda_1}^{\lambda_2} E_{\text{S}}(\lambda) S_{\text{T}}(\lambda) \mathrm{d}\lambda}{\int_{\lambda_1}^{\lambda_2} E_{\text{Ref}}(\lambda) S_{\text{T}}(\lambda) \mathrm{d}\lambda \int_{\lambda_1}^{\lambda_2} E_{\text{S}}(\lambda) S_{\text{R}}(\lambda) \mathrm{d}\lambda} \tag{2}$$

where $E_{\text{Ref}}(\lambda)$ is the reference spectral irradiance, $E_{\text{S}}(\lambda)$ is the source spectral irradiance, $S_{\text{R}}(\lambda)$ is the spectral responsivity of the reference cell, and $S_{\text{T}}(\lambda)$ is the spectral responsivity of the test cell, each as a function of wavelength (λ). The limits of integration λ_1 and λ_2 in the above equation should encompass the range of the reference cell and the test-device spectral re-

sponses, and the simulator and reference spectra should encompass λ_1 and λ_2 to avoid error.[43] A matched PV reference cell is typically used as the reference detector and a solar simulator is used as the light source to minimize the deviation of M from unity. Only the normalized values and not the absolute of $E_S(\lambda)$, $S_R(\lambda)$, and $S_T(\lambda)$ need to be measured for Equation 2. Equation 2 is valid for any thermal or PV detector or light source, provided none of the integrals are zero. In the extreme case of a laser as the light source and a thermal detector with a wavelength-independent responsivity, the uncertainty in M is dominated by the uncertainty in the spectral responsivity.

The total effective irradiance of the light source (E_{eff}), which is the total irradiance seen by the cell, can be determined from the short-circuit current of the reference cell under the source spectrum ($I^{R,S}$) from the equation

$$E_{eff} = \frac{I^{R,S} M}{CN} \tag{3}$$

where CN is the calibration number (in units of $AW^{-1}m^2$) for the instrument used to measure the incident irradiance. E_{eff} is different from E_{tot} in Equation 1, since E_{tot} usually refers to the total irradiance integrated over the entire spectrum, and not just the part of the spectrum the cell responds to. Both E_{eff} and E_{tot} are derived from integrating $E_S(\lambda)$ over an appropriate range of wavelength. The short-circuit current of a test cell ($I^{T,R}$) at the reference total irradiance (E_{Ref}) is given as[32,42]

$$I^{T,R} = \frac{I^{T,S} E_{Ref} CN}{I^{R,S} M} \tag{4}$$

where $I^{T,S}$ is the short-circuit current of a test cell measured under the source spectrum. Once M is known, the simulator is adjusted so that E_{eff} is equal to E_{Ref}, or

$$I^{T,R} = \frac{I^{R,R} I^{T,S}}{I^{R,S} M} \tag{5}$$

where $I^{R,R}$ is the calibrated short-circuit current of the reference cell under the reference spectrum and total irradiance. This is the standard simulator-based calibration procedure. The primary reference-cell calibration methods are described elsewhere.[33] The primary terrestrial procedures employed by the US at NREL follow Equations 1–5 with a primary absolute cavity radiometer as the reference detector, and direct normal sunlight as the source spectrum.

2.1. Spectral-Responsivity Measurements

The calibration procedure described in the above section requires the knowledge of M for a given light source and a given test-cell/reference-cell combination. This, in turn, requires the spectral irradiance of the light source and the spectral responsivities of the test and reference cells. The spectral responsivity, $S(\lambda)$, is calculated from the quantum efficiency, $QE(\lambda)$, by[33]

$$S(\lambda) = \frac{q\lambda}{hc} QE(\lambda) \tag{6}$$

where the constant term q/hc equals 8.0655×10^5 for wavelength in units of meters and $S(\lambda)$ in units of AW^{-1}. The term $QE(\lambda)$ is basically the number of electron–hole pairs generated per incident photon in the device multiplied by 100. To calculate M for various test-cell/reference-cell combinations, we selected four test cells and two reference cells. The reference cells were a monocrystalline silicon diode (Newport 818-SL) and a Schott visible-color glass-filtered (KG5 color filtered) Si diode (Hamamatsu S1133). As described in the Experimental section, the four different types of test cells had the following active layers: i) MEH-PPV:PCBM; ii) P3HT:PCBM(DCB); iii) P3HT:PCBM(CB); and iv) CuPc/C_{60}/BCP (BCP: bathocuproine). These four device structures represent the most common types of organic solar cells being investigated at various research laboratories in the world. The spectral responsivities were measured at NREL for all the test and reference cells as per ASTM Standard E1021.[44] The details of the spectral responsivity measurement system at NREL are discussed elsewhere by Emery et al.[45] It is also worthwhile noting that the spectral-responsivity measurements are typically performed at the short-circuit condition (i.e., at zero applied bias), and the relative responsivity is assumed to be the same at maximum-power and short-circuit points. The spectral responsivities of the test cells are plotted versus wavelength in Figure 2a–d under different light-bias intensities. The responsivities of all the cells show a slight dependence on light-bias intensity, although the behavior is different for different materials systems. For CuPc/C_{60}/BCP and P3HT:PCBM(CB), the responsivities show a small decrease when the light-bias intensity is increased from 0 to about 1 sun. On the other hand, the responsivities show a small increase for MEHPPV:PCBM- and P3HT:PCBM(DCB)-based cells with increasing light-bias intensity. However, the light-bias dependence of the responsivity for all the test cells is constant with respect to wavelength, which suggests that the mismatch-factor calculation will be independent of light-bias intensity. It has been reported earlier that the EQE shows a significant reduction when flooded with white light in organic PV cells.[24] The reduction in EQE was attributed to the increased carrier concentration under illumination, which increases recombination and hinders carrier transport due to space-charge build-up within the BHJ structure. The relatively weak dependence of EQE on light-bias intensity for all four types of devices in this work indicates that the carrier transport in the devices is not limited by space-charge build-up.

One important factor that has to be considered when measuring the spectral response of the PV device is the response time of the cell to the chopped light. For some PV cells, such as dye-sensitized solar cells (DSSCs), slow response of the device can result in a significant change in quantum efficiency with chopping frequency, and very low frequencies are required.[46]

ADVANCED FUNCTIONAL MATERIALS

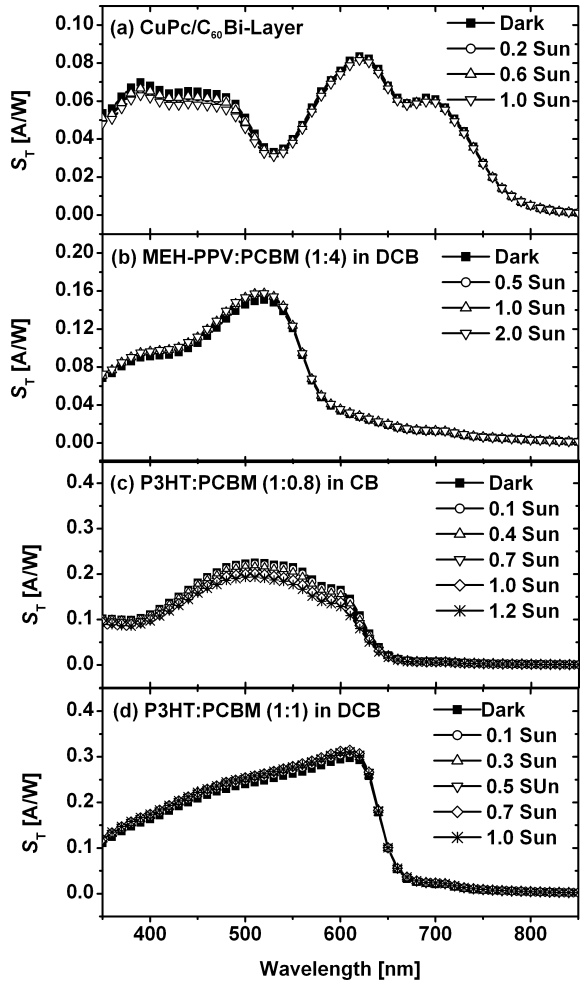

Figure 2. Spectral responsivity, $S_T(\lambda)$, under varying light-bias intensities for test cells with the following active layers: a) CuPc/C_{60}/BCP, b) MEH-PPV:PCBM, c) P3HT:PCBM(CB), and d) P3HT:PCBM(DCB).

However, for polymer solar cells, the response of the device to the incident light is very fast. As shown in Figure 3, for a P3HT:PCBM(DCB) device, the response time is less than a millisecond. As a result, all the cells responded well with chopping frequencies over 150 Hz. These results are in contrast to DSSCs, where EQE measurements are greatly affected by light-bias intensity and chopping frequency. The spectral responsivity measurements and *I–V* characterization of DSSCs has been discussed earlier by Sommeling et al.[46] and Ito et al.[47] Although they are a type of organic solar cell, DSSCs are excluded from discussion in this work, which focuses on solid-state organic solar cells.

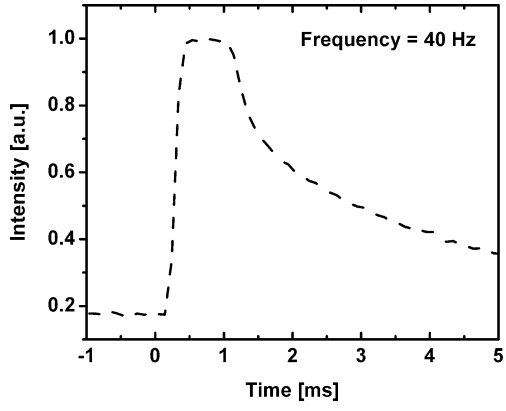

Figure 3. The response of a P3HT:PCBM(DCB) solar cell at a frequency of 40 Hz. At this frequency, the response time of the device is less than a millisecond.

2.2. Light-Source Calibration and Spectral-Mismatch Factor

The relative spectral responsivities of the test and reference cells are an important factor in the solar-simulator calibration procedure. Typically, for crystalline solar cells, the reference cell is made of the same materials and technology as the test device, which results in *M* being close to unity. Of primary importance in a reference cell is the stability in the reference cell's calibration value. For this reason most thin-film organic and inorganic devices use a Si reference cell that may have a filter to improve the spectral match. However, for polymer and small-molecule organic solar cells, it is extremely difficult to fabricate reference cells from the same materials. The reasons for this are the relatively underdeveloped fabrication techniques that lack consistent reproducibility, and poor lifetimes of these devices. Therefore, for the purpose of light-source calibration for organic-solar-cell testing, it is important to select a reference cell whose spectral response matches that of the actual test cells as closely as possible in order to minimize the spectral error that is not being numerically corrected for. The spectral responsivities of the two reference cells we selected are shown in Figure 4a. Also shown for comparison is the spectral response of a thermal detector with a quantum efficiency of unity, which is independent of the wavelength. The response of a thermal detector is very different from that of a PV cell. The unfiltered Si diode shows significant response in the wavelength range 400–1100 nm. However, the response of the Si diode with the KG5 color filter is exhibited in the wavelength range 350–700 nm. Clearly, the responsivity of the latter is similar to the responsivity of our test cells, making it more suitable for use in calibrating the light intensity of the solar simulator. This argument is further supported by calculating the mismatch factor for the four different test cells, using both the reference cells. For the purpose of calculating *M* under AM 1.5 G standard conditions, the reference spectrum used is the AM 1.5 G standard spectrum (IEC 60904),[37] and the source irradiance spectrum is the typical irradiance spectrum of the Oriel 150 W solar simulator with an AM 1.5 G filter (obtained from Newport Corporation). The reference and the source spectra used for calculating *M* are shown in Figure 4b. It should be noted that the spectra of the light sources depend on a number of factors, and the actual irradiance of the light source may be different from the typical spectrum that is shown here. The factors that can affect the irradiance spectrum of the light source are the age of the lamp, optical setting of that particular lamp, and current through the lamp. However, the aim here is to obtain "typical" spectral mismatch-factor values for different test-cell/

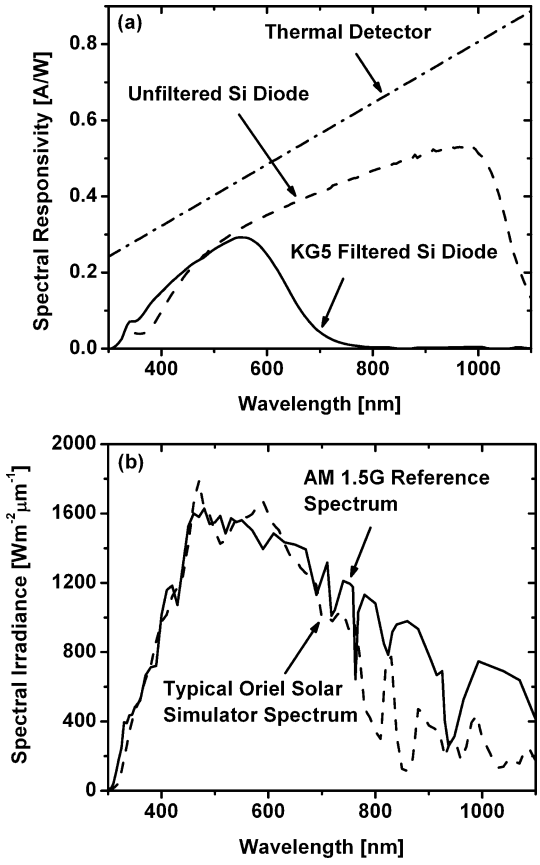

Figure 4. a) Spectral responsivities of two types of reference cells: an unfiltered monocrystalline Si diode and a Si diode with a KG5 color filter. Also shown for comparison is the spectral responsivity for a thermal detector whose quantum efficiency is unity, independent of the wavelength. b) Spectral irradiance data for AM 1.5 G reference spectrum (IEC 60904) [37] and the typical source irradiance for an Oriel 150 W solar simulator with AM 1.5 G filters (obtained from Newport Corporation). Both spectra are plotted for intensities normalized to 100 mW cm^{-2}.

reference-cell combinations using a generic-source spectral irradiance. Obviously, the most accurate M values will be obtained when the actual irradiance spectra of the source is used. The procedure described here is the general method, and the actual irradiance spectra of the source lamp as well as the actual spectral responsivities should be used to calculate the exact M value for a particular test-cell/reference-cell combination. The M values calculated by using the spectral-responsivity data for different test-cell/reference-cell combinations are summarized in Table 1. Using a Si diode with a KG5 color filter as a reference cell for light-source calibration clearly has an advantage over an unfiltered Si diode and a thermal detector. The mismatch-factor values are very close to unity when using a KG5-filtered Si diode reference cell, whereas the mismatch is 31–35 % for the unfiltered Si diode and 33–37 % for the thermal detector. This suggests that when an unfiltered Si diode or a thermal detector is used for calibrating the light-source intensity, possible errors due to spectral mismatch can be as high as 37 %. Once M is known for a specific test-cell/reference-cell combination under the source spectrum, the short-circuit current of the test device under the reference spectrum can be calculated from Equation 4 or 5. In organic solar cells that are not limited by space-charge, such as the ones we have demonstrated here, a linear dependence of short-circuit current density (J_{SC}) with incident-light intensity (I) is observed.[48] On the other hand, the open-circuit voltage (V_{OC}) and fill factor (FF) depend much more weakly on I.[49,50] However, there are bound to be several novel devices that do show a space-charge-limited effect, or other mechanism such as recombination rates, that vary nonlinearly with illumination intensity. Therefore, in order to minimize the error in efficiency calculation, it is extremely important to have M close to unity. Using a reference cell that has a spectral response similar to that of the test cells will result in minimal mismatch. For the KG5 color-filtered reference cell, the mismatch was within ±2 % for all the four test cells in this study. Mismatch factors have been used in the past to correct the efficiency values for polymer BHJ solar cells.[11,12,35] We mentioned earlier that the actual irradiance of a light source depends on several factors, one of which is the age of the lamp. As a result, the spectral mismatch would change with the age of the solar simulator's lamp. Figure 5 shows the spectral-mismatch factor for a P3HT:PCBM(DCB) test cell as a function of lamp age. The light source is a Spectrolab X25 solar simulator operating at one sun. We used two different reference cells (unfiltered and KG5-filtered Si diodes)

Table 1. Spectral-mismatch factors calculated with respect to the AM 1.5 G reference spectrum (IEC 60904) [37] for various test-cell/reference-cell combinations. The spectral responsivities of the test cells used for the data shown here were measured under a light bias of ~1 sun. The effect of light-bias intensity on the spectral-mismatch factor was negligible (< 0.1 %).

	Mismatch factors for different reference cells		
Test-cell type	KG5 color filtered	Unfiltered	Thermal detector
MEHPPV:PCBM	0.99	1.32	1.35
CuPc/C_{60}/BCP	0.98	1.31	1.33
P3HT:PCBM(CB)	1.01	1.35	1.37
P3HT:PCBM(DCB)	1.01	1.35	1.37

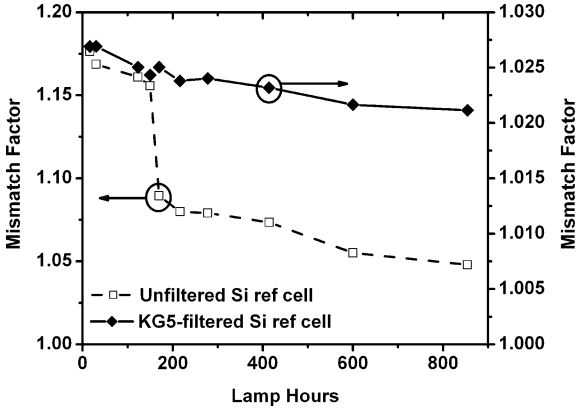

Figure 5. The change in spectral-mismatch factor as a function of lamp age for a P3HT:PCBM(DCB) test cell. The mismatch is calculated for two reference cells: unfiltered and KG5-filtered Si diodes. The light source was a one-sun Spectrolab X25 solar simulator.

ADVANCED FUNCTIONAL MATERIALS

for calculating M. For the unfiltered Si reference cell the mismatch varied by more than 10 % over 900 h. However, for the KG-filtered mono-Si cell, the mismatch varied by only 1 % over 900 h. This not only shows the variation in M with lamp age, but again demonstrates the advantage of using a KG5-filtered Si diode as a reference cell.

2.3. *I–V* Characteristics

The focus of this paper is on spectral-mismatch factor rather than on the device performance, because many factors, such as organic materials source, purity, and detailed device fabrication conditions, can have a significant impact on the device performance. The *I–V* curves were measured at NREL using a Spectrolab X25 solar simulator, whose intensity was set with a primary reference cell and a spectral correction factor to give the performance under the AM 1.5 global reference spectrum (IEC 60904).[37] The measurement was performed under SRC, i.e., 100 mW cm^{-2} irradiance, AM 1.5 global reference spectrum, and 25 °C cell temperature. The test cells were kept at 25.0 ± 1.0 °C during the measurement, where test cells were exposed to simulator irradiation for a measurement time of ~ 1 s. The *I–V* characteristics of the test cells are shown in Figure 6. The device area for each cell was measured using an optical microscope. The device with P3HT:PCBM(DCB) shows the best performance, with a PCE of 4.01 % (J_{SC} = 9.996 mA cm^{-2}; V_{OC} = 0.6028 V; FF = 66.60 %). However, the efficiency of the device with P3HT:PCBM(CB) is only 2.19 % (J_{SC} = 6.697 mA cm^{-2}; V_{OC} = 0.6149 V; FF = 53.14 %). Clearly, the reasons for lower performance are lower current-density and FF values, as V_{OC} is more or less unchanged. Lower J_{SC} is a result of the relatively lower EQE for the P3HT:PCBM (1:0.8) blend obtained from the CB solution, as discussed earlier (see Fig. 2). The MEHPPV:PCBM (1:4, from DCB) device has a PCE of 1.66 % (J_{SC} = 4.366 mA cm^{-2}; V_{OC} = 0.8749 V; FF = 43.46 %), and the CuPc/C_{60}/BCP device has a PCE of only 1.03 % (J_{SC} = 4.2198 mA cm^{-2}; V_{OC} = 0.5706 V; FF = 42.61 %). Even though the processing is the same, the significant difference in the performance of the two types of P3HT:PCBM devices is attributed to the morphology difference between the two active layers when spin-cast from DCB and CB. The boiling point of DCB is significantly higher than that of CB; as a result, the drying time of the film by evaporation of the solvent is slower for films spin-cast from DCB. An increased time will allow the films to achieve a higher level of ordering by self-organization of polymer chains in the active layer.[18] The obvious difference in the shape of spectral response as well as EQE of the two P3HT:PCBM-based solar cells fabricated by different methods is worth noting. The EQE of the slowly grown device has an almost constant response from 500 to 600 nm,[18] which is different from that of other reported P3HT:PCBM solar cells where EQE peaks at ca. 500 nm and consistently decreases at longer wavelengths.[15,51] The enhanced red-region spectral response is believed to be a result of improved polymer-chain ordering from the slow growth process.

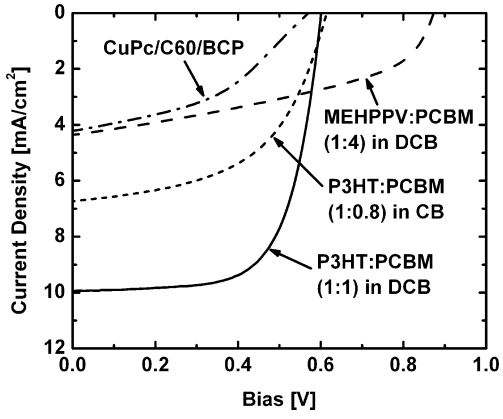

Figure 6. The *I–V* characteristics for four test cells under 100 mW cm^{-2} AM 1.5 G standard spectrum after mismatch correction.

2.4. Device Area

To accurately determine the current density through the device, it is essential to correctly measure the device area (the total frontal area of the cell including the area covered by the grids and contacts).[32,52] Usually, the device area is chosen as the area defined by the shadow mask used for evaporating the top contact. The area of the peripheral contacts to the substrate or superstrate in thin-film solar cells often exceeds the device area and is not well defined. For this reason, the peripheral thin-film contact area is not usually included as part of the total area. An important factor that can result in significant errors in the estimation of the area is the shadow effect arising from evaporating successive layers from multiple sources. One such example is the Ca/Al top electrode used in our study for all three polymer BHJ solar cells. Figure 7 shows an optical microscopy image of copper (30 nm) and gold (40 nm) metal layers successively evaporated onto an indium tin oxide (ITO) substrate. The two metals were chosen because the difference in film color makes it easier to see the shadow effect when observed under an optical microscope. For six different films prepared in this manner, the actual device area (defined by the overlapped area of the Cu and Au films) was 91 ± 3 % of the total area. It is clear that the shadow effect can therefore result

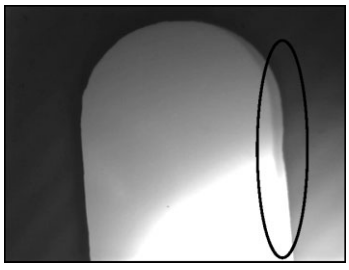

Figure 7. The grayscale optical microscope image of Cu and Au layers evaporated on an ITO substrate to demonstrate the shadow effect. The incomplete overlap of the two metallic films which results in a reduction in the device area is highlighted by the black oval.

in up to a 12 % error in current-density values. The device area for all four types of test cells that were fabricated in this study is 10.7 ± 0.2 mm^2. The device area for each cell was measured separately in order to calculate current-density and efficiency values for that device. The shadow effect can be reduced significantly by adjusting the mask orientation in such a way that the device (finger) length direction is parallel to the connecting line between the sources. The device area for each device should be measured separately to correct the values of current density.

3. Conclusions

The methods for accurately rating the performance of organic solar cells have been presented. Some of the important issues with respect to these devices were discussed, such as spectral responsivity and its behavior with light-bias intensity, dependence of the device parameters on the incident-light intensity, and calculation and application of spectral-mismatch factor for efficiency correction. Four different types of test cells and two reference cells were selected for calculating mismatch factors with respect to the AM 1.5 G reference spectrum. These typical spectral-mismatch factors provide guidance in estimating spectral mismatch in different solar-cell testing settings. The main aim of this work is to motivate the organic-solar-cell community to adopt standards similar to those used for inorganic solar cells for rating device performance.

4. Experimental

In this work, two types of organic solar cells were fabricated: polymer/fullerene BHJ and small-molecule-based bilayer solar cells. The polymer PV devices were fabricated by spin-coating a blend of polymer:fullerene sandwiched between a transparent anode and a cathode. The anode consisted of glass substrates precoated with indium tin oxide (ITO) modified by spin-coating a PEDOT:PSS layer, and the cathode consisted of Ca (ca. 25 nm) capped with Al (ca. 80 nm). Before device fabrication, the ITO (ca. 150 nm)-coated glass substrates were cleaned by ultrasonic treatment in detergent, deionized water, acetone, and isopropyl alcohol sequentially. A thin layer (ca. 25 nm) of PEDOT:PSS (Baytron P VP A1 4083) was spin-coated to modify the ITO surface. After baking at 120 °C for 1 h, the substrates were transferred inside a nitrogen-filled glove box (< 0.1 ppm O_2 and H_2O). P3HT (regioregularity 98.5 %, weight-average molecular weight, $M_w \sim 30\,000$ g mol^{-1}, purchased from Rieke Metals, Inc.; used as received) and MEH-PPV (purchased from Organic Vision, Inc.; used as received) were blended with PCBM (purchased from Nano-C, Inc.; used as received) to obtain the active layer. Two different P3HT:PCBM blend solutions were prepared—one with a 1:1 weight ratio (20 mg mL^{-1} P3HT) in DCB and one with a 1:0.8 weight ratio (10 mg mL^{-1} P3HT) in CB—to fabricate two types of devices named P3HT:PCBM(DCB) and P3HT:PCBM(CB), respectively. P3HT:PCBM(DCB) devices were fabricated by spin-coating the blend at 600 rpm for 60 s. After slow growth, the films were thermally annealed at 110 °C for 10 min in nitrogen atmosphere before evaporating the cathodes [17,18]. For P3HT:PCBM(CB) films, the spin speed was 700 rpm (60 s), and thermal annealing was done at 150 °C for 30 min post production [20]. For the MEH-PPV:PCBM devices, a solution of 1:4 weight ratio (4 mg mL^{-1} MEH-PPV) in DCB was used to spin-cast the active layer. For small-molecule-based devices, CuPc was selected as the active layer. The devices were fabricated by thermally evaporating successive layers of CuPc (20 nm), C_{60} (30 nm), BCP (10 nm), and Al (100 nm) onto the ITO/PEDOT:PSS substrates under a vacuum of 10^{-6} Torr (1 Torr ≈ 133 Pa).

Received: June 5, 2006
Final version: July 22, 2006
Published online: September 12, 2006

[1] C. J. Brabec, N. S. Sariciftci, J. C. Hummelen, *Adv. Funct. Mater.* **2001**, *11*, 15.
[2] P. Peumans, A. Yakimov, S. R. Forrest, *J. Appl. Phys.* **2003**, *93*, 3693.
[3] C. J. Brabec, V. Dyakonov, J. Parisi, N. S. Sariciftci, in *Organic Photovotlaics: Concepts and Realization*, Springer, Berlin **2003**.
[4] K. M. Coakley, M. D. McGehee, *Chem. Mater.* **2004**, *16*, 4533.
[5] C. J. Brabec, *Sol. Energy Mater. Sol. Cells* **2004**, *83*, 273.
[6] S. S. Sun, N. S. Sariciftci, in *Organic Photovoltaics: Mechanisms, Materials and Devices*, CRC Press, Boca Raton, FL **2005**.
[7] G. Yu, J. Gao, J. C. Hummelen, F. Wudl, A. J. Heeger, *Science* **1995**, *270*, 1789.
[8] N. S. Saraciftci, L. Smilowitz, A. J. Heeger, F. Wudl, *Science* **1992**, *258*, 1474.
[9] C. W. Tang, *Appl. Phys. Lett.* **1986**, *48*, 183.
[10] L. J. Lutsen, P. Adriaensens, H. Becker, A. J. Van Breemen, D. Vanderzande, J. Gelan, *Macromolecules* **1999**, *32*, 6517.
[11] S. E. Shaheen, C. J. Brabec, F. Padinger, T. Fromherz, J. C. Hummelen, N. S. Sariciftci, *Appl. Phys. Lett.* **2001**, *78*, 841.
[12] M. M. Wienk, J. M. Kroon, W. J. H. Verhees, J. Knol, J. C. Hummelen, P. A. van Hal, R. A. J. Janssen, *Angew. Chem. Int. Ed.* **2003**, *42*, 3371.
[13] T. Chen, R. D. Rieke, *J. Am. Chem. Soc.* **1992**, *114*, 10 087.
[14] R. D. McCullough, R. D. Lowe, M. Jayaraman, D. L. Anderson, *J. Org. Chem.* **1993**, *58*, 904.
[15] F. Padinger, R. S. Rittberger, N. S. Sariciftci, *Adv. Funct. Mater.* **2003**, *13*, 85.
[16] D. Chirvase, J. Parisi, J. C. Hummelen, V. Dyakonov, *Nanotechnology* **2004**, *15*, 1317.
[17] G. Li, V. Shrotriya, Y. Yao, Y. Yang, *J. Appl. Phys.* **2005**, *98*, 043 704.
[18] G. Li, V. Shrotriya, J. Huang, Y. Yao, T. Moriarty, K. Emery, Y. Yang, *Nat. Mater.* **2005**, *4*, 864.
[19] M. Reyes-Reyes, K. Kim, D. L. Carroll, *Appl. Phys. Lett.* **2005**, *87*, 083 506.
[20] W. L. Ma, C. Y. Yang, X. Gong, K. Lee, A. J. Heeger, *Adv. Funct. Mater.* **2005**, *15*, 1617.
[21] N. S. Sariciftci, D. Braun, C. Zhang, V. I. Sradnov, A. J. Heeger, G. Stucky, F. Wudl, *Appl. Phys. Lett.* **1993**, *62*, 585.
[22] S. Alem, R. de Bettignies, J.-M. Nunzi, M. Cariou, *Appl. Phys. Lett.* **2004**, *84*, 2178.
[23] J. C. Hummelen, B. W. Knight, F. LePeq, F. Wudl, J. Yao, C. L. Wilkins, *J. Org. Chem.* **1995**, *60*, 532.
[24] P. Peumans, S. Uchida, S. R. Forrest, *Nature* **2003**, *425*, 158.
[25] J. Xue, S. Uchida, B. P. Rand, S. R. Forrest, *Appl. Phys. Lett.* **2004**, *85*, 5757.
[26] F. Yang, M. Shtein, S. R. Forrest, *Nat. Mater.* **2005**, *4*, 37.
[27] J. Drechsel, B. Männig, F. Kozlowski, D. Gebeyehu, A. Werner, M. Koch, K. Leo, M. Pfeiffer, *Thin Solid Films* **2004**, *451–452*, 515.
[28] J. Drechsel, B. Männig, D. Gebeyehu, M. Pfeiffer, K. Leo, H. Hoppe, *Org. Electron.* **2004**, *5*, 175.
[29] C.-W. Chu, Y. Shao, V. Shrotriya, Y. Yang, *Appl. Phys. Lett.* **2005**, *86*, 243 506.
[30] S. Yoo, B. Domercq, B. Kippelen, *Appl. Phys. Lett.* **2004**, *85*, 5427.
[31] K. Emery, C. Osterwald, *Sol. Cells* **1986**, *17*, 253.
[32] K. Emery, C. Osterwald, in *Current Topics in Photovoltaics*, Vol. 3, Academic, London **1988**, Ch. 4.
[33] K. Emery, in *Handbook of Photovoltaic Science and Engineering* (Eds: A. Luque, S. Hegedus), Wiley, Chichester, UK **2003**, Ch. 16.
[34] J. Rostalski, D. Meissner, *Sol. Energy Mater. Sol. Cells* **2000**, *61*, 87.

ADVANCED FUNCTIONAL MATERIALS

[35] J. M. Kroon, M. M. Wienk, W. J. H. Verhees, J. C. Hummelen, *Thin Solid Films* **2002**, *403–404*, 223.

[36] Standard IEC 60904-3, Measurement Principles for Terrestrial PV Solar Devices with Reference Spectral Irradiance Data, International Electrotechnical Commission, Geneva, Switzerland.

[37] Standard IEC 60904-1, Photovoltaic devices Part 1: Measurement of Photovoltaic Current-Voltage Characteristics, International Electrotechnical Commission, Geneva, Switzerland.

[38] ASTM Standard G159, Standard Tables for Reference Solar Spectral Irradiances: Direct Normal and Hemispherical on 37° Tilted Surface, American Society for Testing and Materials, West Conshocken, PA, USA.

[39] ASTM Standard G173, Standard Tables for Reference Solar Spectral Irradiances: Direct Normal and Hemispherical on 37° Tilted Surface, American Society for Testing and Materials, West Conshocken, PA, USA.

[40] Standard ASTM E948, Standard Test Method for Electrical Performance of Non-Concentrator Photovoltaic Cells Using Reference Cells, American Society for Testing and Materials, West Conshocken, PA, USA.

[41] K. Emery, C. R. Osterwald, T. W. Cannon, D. R. Myers, J. Burdick, T. Glatfelter, W. Czubatyj, J. Yang, in *Proc. 18th IEEE Photovoltaic Specialist Conf.*, IEEE, New York **1985**, p. 623.

[42] C. R. Osterwald, *Sol. Cells* **1986**, *18*, 269.

[43] H. Field, K. Emery, in *Proc. 23rd IEEE Photovoltaic Specialist Conf.,* IEEE, New York **1993**, p. 1180.

[44] Standard ASTM E1021, Standard Test Methods for Measuring Spectral Response of Photovoltaic Cells, American Society for Testing and Materials, West Conshocken, PA, USA.

[45] K. Emery, D. Dunlavy, H. Field, T. Moriarty, in *Proc. 2nd World Conf. and Exhibition on Photovoltaic Solar Energy Conversion,* European Commission, **1998**, p. 2298.

[46] P. M. Sommeling, H. C. Rieffe, J. A. M. van Roosmalen, A. Schönecker, J. M. Kroon, J. A. Wienke, A. Hinsch, *Sol. Energy Mater. Sol. Cells* **2000**, *62*, 399.

[47] S. Ito, H. Matsui, K. Okada, S. Kusano, T. Kitamura, Y. Wada, S. Yanagida, *Sol. Energy Mater. Sol. Cells* **2004**, *82*, 421.

[48] L. J. A. Koster, V. D. Mihailetchi, R. Ramaker, P. W. M. Blom, *Appl. Phys. Lett.* **2005**, *86*, 123 509.

[49] V. Dyakonov, *Thin Solid Films* **2004**, *451–452*, 493.

[50] S. Yoo, B. Domercq, B. Kippelen, *J. Appl. Phys.* **2005**, *97*, 103 706.

[51] J. Y. Kim, S. H. Kim, H.-H. Lee, K. Lee, W. Ma, X. Gong, A. J. Heeger, *Adv. Mater.* **2006**, *18*, 572.

[52] Standard ASTM E1328, Standard Terminology Relating to Photovoltaic Solar Energy Conversions, American Society for Testing and Materials, West Conshocken, PA, USA.